

# Manipulating Charge Transfer States in BODIPYs: A Model Strategy to Rapidly Develop Photodynamic Theragnostic Agents

Josué Jiménez,<sup>[a],§</sup> Ruth Prieto-Montero,<sup>[b],§</sup> Beatriz L. Maroto,<sup>[a]</sup> Florencio Moreno,<sup>[a]</sup> María J. Ortiz,<sup>[a]</sup> Ainhoa Oliden-Sánchez,<sup>[b]</sup> Iñigo López-Arbeloa,<sup>[b]</sup> Virginia Martínez-Martínez<sup>\*[b]</sup> and Santiago de la Moya<sup>\*[a]</sup>

**Abstract:** On the basis of a family of BINOL-based O-BODIPY dyes, it is demonstrated that chemically manipulating the chromophoric push-pull character, by playing with the electron-donating capability of the BINOL moiety (BINOL vs. 3,3'-dibromoBINOL) and with the electron acceptor ability of the BODIPY core (alkyl substitution degree), is a workable strategy to finely balance fluorescence (singlet-state emitting action) vs. capability to photogenerate cytotoxic reactive oxygen species (triplet-state photosensitizing action). It is also shown that the promotion of a suitable CT character in the involved chromophore upon the excitation enhances the probability of the intersystem crossing (ISC) phenomenon, which is required to populate the triple state enabling singlet oxygen production. The reported strategy opens up new perspectives for the rapid development of smarter agents for photodynamic theragnosis, including heavy-atom-free agents, from a selected starting organic-fluorophore precursor.

Theragnosis, consisting in the simultaneous diagnosis and treatment by a single biocompatible chemical system (*i.e.*, the theragnostic agent), has emerged as a promising medical practice, mainly in the fight against cancer. This is due to the advantageous opportunities that theragnosis offers: it increases the success of the therapy by the aid of the *in-situ* visualization of the lesion to be treated.<sup>2</sup> In fact, theragnosis outstands as one of the most promising practices in modern precision medicine.<sup>2</sup> However, combining diagnosis and treatment abilities in a single biocompatible system is not an easy task. Therefore, the chemical development of smarter theragnostic agents is one of the most challenging objectives in biomaterials science.<sup>3</sup>

Among all the different theragnostic approaches,<sup>1-3</sup> those based on diagnosis by fluorescence bioimaging and medical treatment by photodynamic therapy (PDT), must be highlighted.<sup>4</sup> The benefit of this approach is that it can be performed by the simplest theragnostic agent: a small monochromophoric organic dye able to fluoresce and to photogenerate cytotoxic reactive oxygen species (ROS) from the same chromophore. In other

words, a fluorescent ROS photosensitizer (ROS-PS). This type of theragnostic agent has the additional advantage of its low structural complexity, which is key to speed up the development of the smarter (more efficient and less toxic) agents demanded for advanced medical treatments. However, obtaining such fluorescent ROS-PS agent is not easy, since it requires opposite photonic capabilities yet coming from the same chromophore (the higher the fluorescence efficiency is, the lower the ROS photosensitizing action, and *vice versa*; see Figure 1).<sup>6</sup> Consequently, both properties need to be properly balanced in the molecular design to reach an efficient agent with the required dual photonic action.<sup>5</sup>

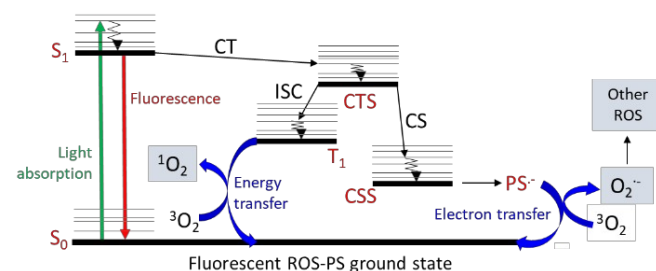


**Figure 1.** Jablonsky diagram showing fluorescence (red) competing with ROS generation (blue) upon light absorption (green) in a monochromophoric fluorescent ROS-PS. A properly stabilized charge transfer state (CTS), populated from the  $S_1$  state, is proposed to enable intersystem crossing (ISC) towards a  $T_1$  state able to generate  $^1O_2$  via energy transfer to the ground state (triplet) of molecular oxygen. Other ROS can be competitively formed by electron transfer from electron-rich PS-based species (*e.g.* the radical anion  $PS^-$ ) to molecular oxygen. These activated species should be mainly formed from a more reactive and polarized charge separation state (CSS).

To date, the most important strategy to construct ROS-PSs is selecting a highly fluorescent monochromophoric organic dye and, then, chemically attaching heavy atoms to its structure, mainly halogenated atoms or heavy transition metals.<sup>5a,d</sup> These atoms promote an efficient population of the triplet excited state ( $T_1$ ) of the dye required to generate singlet oxygen ( $^1O_2$ ), by enabling intersystem crossing (ISC by heavy atom effect) from its first singlet excited state ( $S_1$ ).<sup>6,7c</sup> Highly fluorescent BODIPY (boron dipyrromethene) dyes outstand in this heavy-atom strategy.<sup>5a,7</sup> Unfortunately, heavy atoms usually lead to fast  $T_1 \rightarrow S_0$  ISC, showing relatively short-lived triplet states, which limits their use in PDT.<sup>8</sup> Besides, heavy atoms can increase the toxicity of the agent in the absence of light irradiation (dark toxicity), diminishing the dye biocompatibility.<sup>9</sup> Trying to overcome these drawbacks, some heavy-atom-free ROS-PSs based on organic dye have been recently reported.<sup>5b,7c,10</sup> Although the origin of the photosensitizing capability in these dyes is still controverted, it has been suggested that structural distortion<sup>10g,10h</sup> or charge transfer (CT)<sup>10e,f,11</sup> promotion upon the excitation can be involved in the enhancement of the probability of the ISC required to generate  $^1O_2$  (Figure 1). In this context, turning on a charge transfer state

[a] J. Jiménez, Prof. B. L. Maroto, Prof. F. Moreno, Prof. M. J. Ortiz, Prof. S. de la Moya  
Departamento de Química Orgánica, Facultad de Ciencias Químicas, Universidad Complutense de Madrid  
Ciudad Universitaria s/n, 28040, Spain  
santmoya@ucm.es

[b] R. Prieto-Montero, A. Oliden-Sánchez, Prof. I. López-Arbeloa, Prof. V. Martínez-Martínez  
Departamento de Química Física, Facultad de Ciencias y Tecnología, Universidad del País Vasco EHU. 48080, Spain  
Virginia.martinez@ehu.es

§ These authors contributed equally to this work.

Supporting information for this article is given via a link at the end of the document.

(CTS) has been recently used to switch between fluorescence and ROS generation.<sup>12a</sup> Therefore, manipulating CTSs in small organic dyes could be an interesting strategy in the development of smarter photodynamic therapeutic agents, including heavy-atom-free ones. By this strategy, it should be possible to rapidly find a privileged structure with the most proper balance between ROS photoproduction and fluorescence. Herein, we demonstrate the utility of chemically manipulating CTSs as a useful strategy to develop fluorescent ROS-PSs for photodynamic therapy.

To this end, we selected four accessible and highly fluorescent *F*-BODIPY precursors (**1-4** in Figure 2), which were chemically manipulated to tune their ability to populate CTSs upon excitation. Then, they were photophysically characterized to study their capability to act as fluorescent ROS-PSs. The said chemical manipulation was to covalently link the oxygen atoms of a BINOL (1,1'-binaphth-2-ol) or 3,3'-dibromoBINOL moiety to the boron atom of **1-4** (substitution of the fluorines by a BINOL moiety), to generate the corresponding *O*-BODIPY dyes (**1a-4a** and **1b-4b**, respectively; see Figure 2). This simple chemical transformation was selected due to the known differential ability of BODIPYs **1**, **1a** and **1b**, previously studied by us, to undergo charge transfer (CT) upon excitation.<sup>13</sup> Thus, the at-boron functionalization of BODIPYs with BINOL moieties promotes a fluorescence-quenching CT process.<sup>13</sup> Such CT can be efficiently tuned by manipulating the substitution pattern in the BODIPY-BINOL system, particularly by diminishing the electron-donating capability of the BINOL moiety (using bromine as electron-withdrawing substituent at BINOL), or by enhancing the electron-acceptor ability of the BODIPY core (e.g., by diminishing the number of alkyl groups at BODIPY).<sup>13</sup>

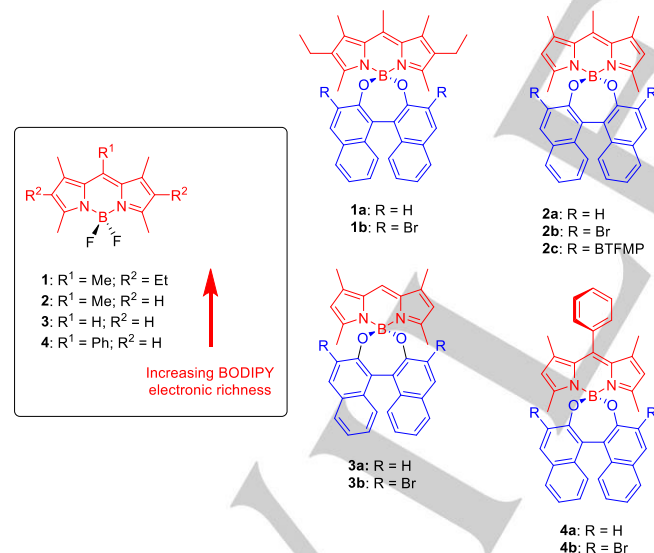


**Figure 2.** Selected BINOL-based *O*-BODIPYs, as well as parent *F*-BODIPYs (inset). BODIPY and BINOL-based moieties are highlighted in red and blue, respectively. BTFMP: 3,5-bis(trifluoromethyl)phenyl.

Known *O*-BODIPYs **1a**,<sup>14</sup> **1b**,<sup>15</sup> and **4a**<sup>16</sup> were prepared from the corresponding parent *F*-BODIPY and BINOL or 3,3'-dibromoBINOL, following the described procedures based on standard  $AlCl_3$  activation of the fluorine substitutions. The same method was successfully used to prepare **2a-b**, **3a-b** and **4b** (see Figure S1 and synthetic details in Supporting Information, SI).

BINOLated *O*-BODIPYs **2a-4a** were expected to populate CTSs with higher probability than their 3,3'-dibromoBINOLated counterparts **2b-4b** (see Figure 2), analogously to that occurring in the couple **1a/1b**.<sup>13</sup> Accordingly, among the selected dyes, **1b** should exhibit the lowest probability to populate CTS upon excitation, since this dye is based on electron-poor 3,3'-dibromoBINOL and the electron-richer BODIPY core (note peralkylation injecting electronic density into the BODIPY core of **1b**). Oppositely, **4a**, based on electron-rich BINOL and the electron-poorest BODIPY core (note the lower degree of BODIPY alkylation together with the presence of an orthogonal, electron-withdrawing, phenyl group), should exhibit the highest CT probability in all the studied BINOL-based *O*-BODIPYs in this work.

To test the expected different ability of **1-4**, **1a-4a** and **1b-4b** to undergo CT, fluorescence dependence on solvent polarity was studied for each dye (see Table S1 in SI). The ability of these dyes to fluoresce was accounted by their fluorescence quantum yields ( $\phi$  in solvents of different polarity, whereas their ability to populate a ROS-forming triplet state was estimated by the corresponding singlet-oxygen ( $^1O_2$ ) quantum yield ( $\phi$ ) in chloroform (see Table 1, Table S1 and Figures S2-S5 in SI). It must be noted here that competitive formation of other ROS (see the electron-transfer mechanism in Figure 1) is considered negligible under the experimental conditions chosen to quantify the photoproduction of  $^1O_2$  (diluted non-aqueous media). Thus, according to previous works,<sup>17,18</sup> the predominant ROS-forming mechanism for all the herein studied BODIPYs, under the selected experimental conditions, should be energy transfer from the triplet state to molecular oxygen, to form  $^1O_2$ ; nonetheless, formation of small fraction of other ROS (mainly radical anion superoxide,  $O_2^{\cdot-}$ ) cannot be discarded.

The high fluorescence efficiency of **2** and **3** ( $\phi$  ca. 0.9 in chloroform) was much drastically affected upon the substitution of their fluorine atoms by a BINOL in comparison with that occurring in the case of **1**,<sup>13</sup> likely due to the promotion of CT (cf. **1a-3a** vs. **1-3** in Table 1). BINOLation of less fluorescent parent **4** ( $\phi$  ca. 0.6) enables the same effect (cf. **4a** vs. **4** in Table 1). However, the loss of fluorescence efficiency with respect to that of the corresponding parent *F*-BODIPY is significantly less pronounced in **1b-4b**, where the less electron-rich 3,3'-dibromoBINOL moiety is involved, respect to BINOL-based **1a-4a** (see Table 1). Besides, this fluorescence loss follows the tendency **1** < **2** < **3** < **4**, both for the BINOL and the 3,3'-dibromoBINOL series, agreeing with the expected probability of undergoing CT.

To our satisfaction, these results support our starting hypotheses: (1) fluorescence-quenching CT is significantly working in the selected *O*-BODIPYs, but not in the corresponding parent *F*-BODIPYs; (2) the fluorescence efficiency can be finely modulated in these *O*-BODIPYs by chemically manipulating the push-pull character of the involved BODIPY chromophore (proper choice of both BODIPY and BINOL substituents). Thus, **1b**, which was predicted to exhibit the lowest probability to undergo CT, displays the highest fluorescence efficiency among the studied *O*-BODIPYs ( $\phi$  ca. 0.7 in chloroform; see Table 1), whereas **4a**, which was predicted to be endowed with the highest probability to undergo CT, exhibits the lowest emission efficiency under the same experimental conditions ( $\phi = 0.01$ ; see Table 1). Strikingly, BINOLated **2a** is a discordant point in this trend, since its

fluorescence efficiency was found to be almost null under identical conditions, instead of being halfway between those exhibited by **1a** ( $\phi = 0.47$ ) and **3a** ( $\phi = 0.11$ ), as it should be expected (see Table 1).

**Table 1.** Fluorescence ( $\phi$ ) and singlet-oxygen ( $\phi_s$ ) quantum yields for *F*-BODIPYs **1-4**, and *O*-BODIPYs **1a-4a**, **1b-4b** and **2c** in diluted chloroform solution,<sup>[a]</sup> as well as key effects (CT: charge transfer, PET: photoelectron transfer, and heavy atom; see text) affecting these parameters.

	$\phi$	$\phi_s$	CT	PET	Heavy atom
<b>1</b>	0.89	0.00	No	No	No
<b>1a</b>	0.47 <sup>[b]</sup>	0.05	Yes	No	No
<b>1b</b>	0.69 <sup>[b]</sup>	0.11	Yes	No	Yes
<b>2</b>	0.90	0.00	No	No	No
<b>2a</b>	0.06	0.00	No	Yes	No
<b>2b</b>	0.62	0.32	Yes	No	Yes
<b>2c</b>	0.43	0.07	Yes	No	No
<b>3</b>	0.90	0.00	No	No	No
<b>3a</b>	0.11	0.04	Yes	No	No
<b>3b</b>	0.27	0.20	Yes	No	Yes
<b>4</b>	0.60	0.00	No	No	No
<b>4a</b>	0.01	0.00	No	Yes	No
<b>4b</b>	0.16	0.32	Yes	No	Yes

[a] See SI for experimental details. [b] Data collected from ref. 13a.

Trying to shed light on the behaviour of **2a**, we computationally discovered that a photoinduced electron transfer (PET) process is involved in **2a** as the main non-radiative deactivation channel of this dye. Thus, the conducted computations (DFT wB97XD/LanL2DZ; see SI for details) demonstrate that visible light absorption in BINOLated **2a** preferentially implies an electronic transition from HOMO-1 to LUMO, being these orbitals mainly located at the BODIPY core (see Figure S6 in SI). The calculations also show that upon this electronic transition, a PET from the HOMO (mainly located at the BINOL moiety) to the generated low-lying semi-vacant HOMO-1 is thermodynamically feasible (see Figure S6 in SI). This reductive PET explains the dramatic loss of fluorescence observed for **2a** in all the studied solvents (see Table S1 in SI). Therefore, the enabled PET competes with the probability of undergoing CT. Differently, visible light absorption in 3,3'-dibromoBINOLated **2b** is computed to preferentially imply HOMO-to-LUMO electron promotion, being these orbitals localized at the BODIPY core (see Figure S6 in SI). In this case, PET from the low-lying HOMO-1 to the as-generated semi-vacant HOMO is not thermodynamically feasible at room temperature (the involved energy gap is computed to be high: ca. 150 meV; see Figure S6 in SI). Therefore, the expected CT is not turned off by PET in **2b**, as demonstrated by the observed fluorescence dependency on the media polarity exhibited this dye (cf. **2a** and **2b** in Table S1 in SI).

Conducted computations revealed the same behaviour for **4a** (see Figure S6 in SI), switching the CT off by PET.

The promotion of CTS and its competition with PET process has a big impact in the ability to generate ROS in the present BODIPY dyes. In this line, regarding the differential ability to populate the BODIPY triplet state, parent **1-4**, with virtually no ability to undergo CT upon excitation, did not show  $^1\text{O}_2$  photogeneration ( $\phi_s$  almost null in chloroform; see Table 1). As expected, linking the BINOL moiety to the boron atom of these dyes timidly turns on the production of  $^1\text{O}_2$  in CT-enabling **1a** and **3a** ( $\phi_s$  ca. 0.05 in chloroform), but not in PET-enabling **2a** and **4a** (cf. data in Table 1). Therefore, avoiding possible PETs together and properly populating CTS seems to be key to promote the triplet population and, according to our hypothesis, it can be modulated by tuning the stability of the involved CTS. Thus, introducing bromines in the BINOL moiety of **2a**, **3a** and **4a**, to respectively generate **2b**, **3b** and **4b**, increases the CT probability and thus gives place to a significant enhancement of the  $^1\text{O}_2$  photoproduction in chloroform ( $\phi_s$  up to 0.32; see Table 1), which must not only be ascribed to a possible direct  $S_1 \rightarrow T_1$  ISC promoted by heavy atom effect (note the involved bromine atoms), but to the additional key participation of a properly-stabilized CTS intermediating the ISC, due to the electronic effect exerted by the bromine atoms on the push-pull character of the involved BODIPY-BINOL dyad. Actually, 3,3'-dibromoBINOLated *O*-BODIPYs **1b** and **2b** show significantly different ability to produce  $^1\text{O}_2$  under the same experimental conditions (ca three-fold higher for **2b** and **4b** than for **1b** in terms of  $\phi_s$  in chloroform; see Table 1), despite the fact that they involve very similar dibrominated structures (see Figure 2).

The aforementioned results support the influence of the CT probability on the modulation of the triplet population, and its usefulness for designing well-balanced theragnostic agents (e.g., note **2b** exhibiting  $\phi = 0.62$  and  $\phi_s = 0.32$  in Table 1). Moreover, it could be used to design heavy-atom-free PDT agents, too. To support this interesting possibility, and to give more evidence about CT probability modulating triplet population, we designed heavy-atom-free *O*-BODIPY **2c** (see Figure 2). Thus, the electron-donating capability of the BINOL-based moiety of **2c**, which is 3,3'-disubstituted with 3,5-bis(trifluoromethyl)phenyl (BTFMP) groups, should be halfway between that involved in **2a** (based on non-substituted BINOL) and **2b** (based on 3,3'-dibrominatedBINOL), due to the different electron-withdrawing effects exerted by the corresponding groups located at the BINOL 3,3'-positions (H < BTFMP < Br).

BODIPY **2c** was straightforwardly prepared by reacting parent **2** with commercial 3,3'-bis(BTFMP)BINOL, following the used standard procedure to prepare BINOL-based *O*-BODIPYs from *F*-BODIPYs (see Figure S1 and synthetic details in SI). Certainly, both the fluorescence and the capability to generate  $^1\text{O}_2$  of **2c** ( $\phi = 0.43$  and  $\phi_s = 0.07$ ) are between those exhibited by **2a** ( $\phi = 0.06$  and  $\phi_s = 0.00$ ) and **2b** ( $\phi = 0.62$  and  $\phi_s = 0.32$ ), as shown in Table 1. Although a higher  $^1\text{O}_2$  production was expected for **2c**, the obtained experimental results support our hypothesis. Nonetheless, future extra efforts are required to gain a deeper knowledge about the detailed mechanism promoting the triplet state population via CTS. This knowledge should also serve to explain the observed unexpected photophysical features.

Finally, in order to characterize the promoted triplet states, dyes with  $\phi > 5\%$  (i.e., **2b**, **2c**, **3b** and **4b**) were studied by nanosecond transient spectroscopy (see details in SI). The recorded spectra were similar for all the studied compounds (see Figures S7-S11 in SI) and comparable to those previously registered for BODIPYs enabling efficient triplet state population.<sup>5a,7c,19</sup> Remarkably for PDT, all the studied dyes showed relative long triplet lifetimes in the absence of oxygen ( $\tau_0 > 100 \mu\text{s}$ ; see Table S2 in SI), being these values significantly longer than those exhibited by previous iodinated BODIPYs.<sup>5a,7c</sup> Interestingly, by measuring the decay of the triplet transient band at the absorption maximum, in the presence and absence of oxygen, the fractions of excited triplet states quenched by oxygen ( $P^{T_{O_2}}$ ) and the rate constants for the bimolecular oxygen quenching ( $k^{T_{q,O_2}}$ ) could be determined for **2b**, **2c**, **3b** and **4b** at room temperature, resulting in excellent  $P^{T_{O_2}}$  values, near 1, and  $k^{T_{q,O_2}}$  values around of  $1.0 \times 10^9 \text{ M}^{-1} \text{ s}^{-1}$  for all these dyes (see Table S2 in SI).

In summary, we demonstrate the usefulness of manipulating CTSs to balance fluorescence vs. singlet-oxygen photoproduction in purely organic dyes. This can be easily done by chemically tuning the probability of undergoing CT upon the excitation, and constitutes a valuable tool to take into account when developing triplet PSs from bright fluorophores. This strategy is especially relevant when the desired PSs are based on a small monochromophoric organic dye focused to PDT (with long enough triplet-state lifetimes able to generate  $^1\text{O}_2$ , but without involving inherently-toxic metal atoms) and additionally able to exhibit enough fluorescence to aid the desired therapy by bioimaging tracking. Moreover, the demonstrated easiness for tuning the CT probability in BINOL-based O-BODIPYs, by the chemical manipulation of the push-pull character of the involved BINOL-BODIPY dyad, avails the interest of this family of synthetically accessible dyes in the development of new PDT agents. Interestingly, the described CT strategy to develop BODIPY-based PDT agents could be easily extended to other chromophores, organic or not, by using different CT-tuning approaches. This fact opens up new perspectives for the rapid development of smarter, less toxic and more efficient, PDT agents, as well as new triplet PSs for demanded applications beyond ROS photoproduction (e.g., photo-redox catalysis, including  $\text{H}_2$  production by photocatalytic water splitting, photovoltaic applications or photon upconversion by triplet-triplet-annihilation).<sup>20</sup> In this context, the long-lived triplets found for some of the herein reported O-BODIPYs avails a promising future of such simple dyes as triplet PSs for advanced photonics. Finally, further research is in progress in order to gain a deeper insight into the detailed mechanism promoting the triplet state population via CTS in BINOL-based BODIPYs.

## Acknowledgements

Financial support from Ministerio de Ciencia, Innovación y Universidades de España (MAT2017-83856-C3-2-P and MAT2017-83856-C3-3-P) and Gobierno Vasco (IT912-16) is gratefully acknowledged. J.J. and R.P.-M. thank Comunidad de Madrid/UCM and UPV-EHU for respective research contracts.

**Keywords:** Theragnosis • Photodynamic therapy • Singlet oxygen • Triplet modulation • Charge transfer

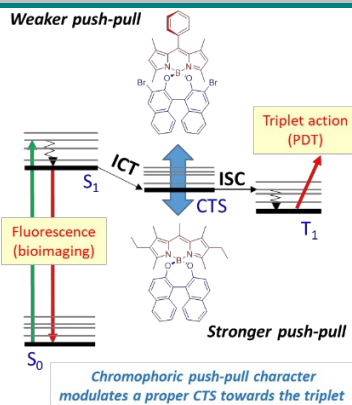
- [1] (a) S. S. Kelkar, T. M. Reineke, *Bioconjugate Chem.* **2011**, *22*, 1879-1903. (b) P. Palekar-Shanbhag, S. V. Jog, M. M. Chogale, S. S. Gaikwad, *Curr. Drug Deliv.* **2013**, *10*, 357-362. (c) *Cancer Theranostics* (Eds.: X. Chen, S. Wong), Academic Press, Oxford, **2014**.
- [2] For example, see: (a) A. Yordanova, E. Eppard, S. Kürpig, R. A. Bundschuh, S. Schönberger, M. Gonzalez-Carmona, G. Feldmann, H. Ahmadzadehfhar, M. Essler, *Onco. Targets Ther.* **2017**, *10*, 4821-4828. (b) *Imaging in Photodynamic Therapy* in Series in Cellular and Clinical Imaging (Eds.: M. R. Hambling, Y. Huang), CRC Press, Boca Raton (USA), **2017**. (c) D. V. Straten, V. Mashayekhi, H. S. De Bruijn, S. Oliveira, D. J. Robinson, *Cancers* **2017**, *9*, 19 (54 pp). (d) H. J. Turner, *Br J Radiol.* **2018**, *91*, 20170893.
- [3] (a) E.-K. Lim, T. Kim, S. Paik, S. Haam, Y.-M. Huh, K. Lee, *Chem. Rev.* **2015**, *115*, 327-394. (b) R. Kumar, W. S. Shin, K. Sunwoo, W. Y. Kim, S. Koo, S. Bhuniya, J. S. Kim, *Chem. Soc. Rev.* **2015**, *44*, 6670-6683. (c) W. Hu, H. Ma, B. Hou, H. Zhao, Y. Ji, R. Jiang, X. Hu, X. Lu, L. Zhang, Y. Tang, Q. Fan, W. Huang, *ACS Appl. Mater. Interfaces* **2016**, *8*, 12039-12047. (d) Y. S. Marfin, A. V. Solomonov, A. S. Timin, E. V. Rummyantsev, *Curr. Med. Chem.* **2017**, *24*, 2745-2772. (e) L. Liu, X. Li, L. Chen, X. Zhang, *Curr. Med. Chem.*, **2018**, *25*, 2987-3000. (f) B. Y. Yang, Chen, J. Shi, *Adv. Mater.* **2019**, *31*, 1802896 (33 pp). (g) X. Tian, S. Liu, J. Zhu, Z. Qian, L. Bai, Y. Pan, *Nanotechnology* **2019**, *30*, 032002. (h) W. Hu, X. Miao, H. Tao, A. Baev, C. Ren, Q. Fan, T. He, W. Huang, P. N. Prasad, *ACS Nano* **2019**, *13*, 12006-12014.
- [4] (a) X. Li, S. Kolemen, J. Yoon, E. U. Akkaya, *Adv. Funct. Mater.* **2017**, *27*, 1604053 (11 pp). (b) B. del Rosal, B. Jia, D. Jaque, *Adv. Funct. Mater.* **2018**, *28*, 1803733 (25 pp). (c) C.-N. Ko, G. Li, C.-H. Leung, D.-L. Ma, *Coord. Chem. Rev.* **2019**, *381*, 79-103.
- [5] For example, see: (a) A. Kamkaew, S. H. Lim, H. B. Lee, L. V. Kiew, L. Y. Chung, K. Burgess, *Chem. Soc. Rev.* **2013**, *42*, 77-88. (b) G. Duran-Sampedro, N. Epelde-Elezcano, V. Martínez-Martínez, I. Esnal, J. Bañuelos, I. García-Moreno, A. R. Agarrabeitia, S. de la Moya, A. Tabero, A. Lazaro, A. Villanueva, M. J. Ortiz, I. López-Arbeloa, *Dyes Pigments*, **2017**, *142*, 77-87. (c) S. Zhen, S. Wang, S. Li, W. Luo, M. Gao, L. G. Ng, C. C. Goh, A. Qin, Z. Zhao, B. Liu, B. Z. Tang, *Adv. Funct. Mater.* **2018**, *28*, 1706945.
- [6] For example, see: P. R. Ogilby, *Chem. Soc. Rev.* **2010**, *39*, 3181-3209.
- [7] (a) T. Yogo, Y. Urano, Y. Ishitsuka, F. Maniwa, T. Nagano, *J. Am. Chem. Soc.* **2005**, *127*, 12162-12163. (b) S. G. Awuahab, Y. You, *RSC Adv.* **2012**, *2*, 11169-11183. (c) J. Zhao, K. Xu, W. Yang, Z. Wang, F. Zhong, *Chem. Soc. Rev.* **2015**, *44*, 8904-8939. (d) X. Miao, W. Hu, T. He, H. Tao, Q. Wang, R. Chen, L. Jin, H. Zhao, Q. Fan, W. Huang, *Chem. Sci.*, **2019**, *10*, 3096-3102.
- [8] E. G. Azenha, A. C. Serra, M. Pineiro, M. M. Pereira, J. Seixas de Melo, L. G. Arnaut, S. J. Formosinho, A. M. d'A Rocha Gonsalves, *Chem. Phys.* **2002**, *280*, 177-190.
- [9] For example, see: J. Zou, Z. Yin, K. Ding, Q. Tang, J. Li, W. Si, J. Shao, Q. Zhang, W. Huang, X. Dong, *ACS Appl. Mater. Interfaces* **2017**, *9*, 32475-32481.
- [10] For example, see: (a) B. Ventura, G. Marconi, M. Broering, R. Kruger, L. Flamigni, *New J. Chem.* **2009**, *33*, 428-438. (b) Z. Yu, Y. Wu, Q. Peng, C. Sun, J. Chen, J. Yao, H. Fu, *Chem. Eur. J.* **2016**, *22*, 4717-4722. (c) J. Zhao, K. Chen, Y. Hou, Y. Che, L. Liu, D. Jia, *Org. Biomol. Chem.* **2018**, *16*, 3692-3701. (d) A. Turksay, D. Yildiz, E. U. Akkaya, *Coord. Chem. Rev.* **2019**, *379*, 47-64. (e) Y. Zhao, R. Duan, J. Zhao, C. Li, *Chem. Commun.* **2018**, *54*, 12329-12332. (f) W. Hu, Y. Lin, X.-F. Zhang, M. Feng, S. Zhao, J. Zhang, *Dyes Pigments* **2019**, *164*, 139-147. (g) T. He, C. Ren, Y. Luo, Q. Wang, J. Li, C. Ye, W. Hu, J. Zhang, *Chem. Sci.* **2019**, *10*, 4163-4168. (h) W. Hu, T. He, H. Zhao, H. Tao, R. Chen, L. Jin, J. Li, Q. Fan, W. Huang, A. Baev, P. N. Prasad, *Angew. Chem.* **2019**, *131*, 11222-11228.
- [11] (a) Z. E. X. Dance, S.M. Mickley, T. M. Wilson, A. B. Ricks, S. M. Amy, M. A. Ratner, M. R. Wasielewski, *J. Phys. Chem. A*, **2008**, *112*, 4194-



4201. (b) A. K. Thomas, H. A. Brown, B. D. Datko, J. A. Garcia-Galvez, J. K. Grey, *J. Phys. Chem. C*, **2016**, *120*, 23230-23238. (c) S. Das, W. G. Thornbury, A. N. Bartynski, M. E. Thompson, S. E. Bradforth, *J. Phys. Chem. Lett.* **2018**, *9*, 3264-3270.
- [12] I. S. Turan, G. Gunaydin, S. Ayan, E. U. Akkaya, *Nature Commun.* **2018**, *9*, 805-813.
- [13] (a) L. Gartzia-Rivero, E. M. Sánchez-Carnerero, J. Jiménez, J. Bañuelos, F. Moreno, B. L. Maroto, I. López-Arbeloa, S. de la Moya, *Dalton Trans.* **2017**, *46*, 11830-11839. (b) J. Jiménez, F. Moreno, B. L. Maroto, T. Cabreros, A. Huy, G. Muller, S. de la Moya, *Chem. Commun.* **2019**, *55*, 1631-1634.
- [14] E. M. Sánchez-Carnerero, F. Moreno, B. L. Maroto, A. R. Agarrabeitia, M. J. Ortiz, B. G. Vo, G. Muller, S. de la Moya, *J. Am. Chem. Soc.* **2014**, *136*, 3346-3349.
- [15] J. Jiménez, L. Cerdan, F. Moreno, B. L. Maroto, I. Garcia-Moreno, J. L. Lunkley, G. Muller, S. de la Moya, *J. Phys. Chem. C* **2017**, *121*, 5287-5292.
- [16] S. Zhang, Y. Wang, F. Meng, C. Dai, Y. Cheng, C. Zhu, *Chem. Commun.* **2015**, *51*, 9014-9017.
- [17] (a) Y.-C. Lai, C.-C. Chang, *J. Mat. Chem. B* **2014**, *2*, 1576-1583. (b) J. Wang, Y. Hou, W. Lei, Q. Zhou, C. Li, B. Zhang, X. Wang, *ChemPhysChem* **2012**, *13*, 2739-2747.
- [18] Y. Vakrat-Haglilili, L. Weiner, V. Brumfeld, A. Brandis, Y. Salomon, B. McLlroy, B. C. Wilson, A. Pawlak, M. Rozanowska, T. Sarna, A. Scherz, *J. Am. Chem. Soc.* **2005**, *127*, 6487-6497.
- [19] (a) W. Wu, X. Cui, J. Zhao, *Chem. Commun.* **2013**, *49*, 9009-9011. (b) D. Liu, Y. Zhao, Z. Wang, K. Xu, J. Zhao, *Dalton Trans.* **2018**, *47*, 8619-8628. (c) Q. Zhou, M. Zhou, Y. Wei, X. Zhou, S. Liu, S. Zhang, B. Zhang, *Phys. Chem. Chem. Phys.* **2017**, *19*, 1516-1525.
- [20] For example see: J. Zhao, W. Wu, J. Sun, S. Guo, *Chem. Soc. Rev.* **2013**, *42*, 5323-5351. Also see refs. 7c and 19b.

## Entry for the Table of Contents (Please choose one layout)

**Chemically tuning** charge transfer states (CTSs) in BODIPYs is revealed as workable strategy to modulate the population of triplet excited states in monochromophoric dyes focused to photodynamic therapy (photodynamic therapy aided fluorescence bioimaging). The strategy could be easily extended to different systems and triplet applications beyond photodynamic therapy.



Josué Jiménez, Ruth Prieto-Montero, Prof. Beatriz L. Maroto, Prof. Florencio Moreno, Prof. María J. Ortiz, Ainhoa Oliden-Sánchez, Prof. Iñigo López-Arbeloa, Prof. Virginia Martínez-Martínez, \* Prof. Santiago de la Moya\*

Page No. – Page No.

**Manipulating Charge Transfer States in BODIPYs: A Model Strategy to Rapidly Develop Photodynamic Theragnostic Agents**